readings, the readout signal was still >60% of the first readout current. It is also possible to refresh the stored charge; for example, a potential pulse sequence of the proper width and magnitude could be coupled with a reading beam pulse to rewrite charge. Here, during the first part of the reading beam pulse, a photodischarge results under short-circuit conditions, and during the second part of the reading beam, a potential pulse is applied to recharge the memory element. By this means, the memory element is refreshed after each reading, in a manner analogous to that used for dynamic random access memories (DRAMs).

The cycle life (the number of cycles of charging and discharging) was tested by applying continuous potential pulses of 0 to +0.5 V (pulse width and interval of 1 ms) to the thin-layer cell under constant irradiation, with the memory element charged at +0.5 V immediately after each readout at 0 V. Even after the cell was charged and discharged >1 billion times (a period of ~12 days), the output current of each reading was essentially identical to the first one. This result suggests the absence of irreversible changes in the film during charging and discharging.

Readout can also be implemented by measuring the voltage produced by the photoinduced charge in the dark. Because no charge flows during a voltage measurement, depletion of the stored signal does not occur in this read mode. Charge generated and stored by a low intensity writing beam (~10 μW cm^{-2}) under a small bias (+0.5 V) was read continuously in the dark with a high input impedance voltmeter (Orion Research Model 701A pH meter) with no perceptible change for >2000 hours. The readout voltage was constant at 20 mV with no evidence of decay. The nature of the trap sites for charge storage in a polycrystalline ZnODEP film is not clear; studies of other systems (8) suggest that they might be crystal defects, grain boundaries, or chemical impurities.

The approach described here for trapping charge in a photoconductive thin film appears promising as a means of information storage. Current state-of-the-art Si-based DRAMs contain 64 megabits (each with a cell size of ~1 to 2 μm^2) and have addressing speeds of 30 to 50 ns (9). We have demonstrated high-density, high-speed writing and long-term stability and cycle life. The structures involved are simple and inexpensive. Although we have used an STM [which has also been recently used in a capacitive mode for charge storage in a nitride-oxide-silicon (NOS) system (10)] to write and read data, high-resolution lithographics might also be useful in the fabrication of memory devices based on this system. The experimental results reported here were obtained with ZnODEP, but other photoconductive materials have shown similar properties in preliminary experiments.

REFERENCES AND NOTES

1. N. V. Joshi, *Photoconductivity: Art, Science, and Technology* (Dekker, New York, 1990).
2. H. Kallmann and B. Rosenberg, *Phys. Rev.* **97**, 1596 (1955).
3. B. Kurrelmeyer, *ibid.* **30**, 893 (1927).
4. V. M. Fridkin and I. S. Zheludev, *Photoelectrets and the Electrophotographic Process* (Consultants Bureau, New York, 1961).
5. B. A. Gregg, M. A. Fox, A. J. Bard, *J. Phys. Chem.* **94**, 1586 (1990).
6. ———, *Chem. Commun.* **1987**, 1143 (1987).
7. ———, *J. Am. Chem. Soc.* **111**, 3024 (1989).
8. J. Simon and J.-J. André, *Molecular Semiconductors* (Springer-Verlag, Berlin, 1985).
9. B. Prince, *Semiconductor Memories* (Wiley, New York, ed. 2, 1991).
10. R. C. Barrett and C. F. Quate, *J. Appl. Phys.* **70**, 2725 (1991).

11. We thank F.-R. F. Fan, P. McCord, and D. Wipf for stimulating discussions and technical assistance. The support of this work by the Texas Advanced Technology Program is gratefully acknowledged.

12 April 1993; accepted 1 July 1993

Electron Diffraction and Imaging of Uncompressed Monolayers of Amphiphilic Molecules on Vitreous and Hexagonal Ice

J. Majewski, L. Margulis, D. Jacquemain, F. Leveiller, C. Böhm, T. Arad, Y. Talmon, M. Lahav, L. Leiserowitz*

A new approach is described for probing domains of ordered self-assemblies of amphiphilic monolayers at the aqueous solution interface. The method has potential importance for the study of membrane structure, Langmuir-Blodgett films, and nucleation processes of two- and three-dimensional crystals. Electron diffraction (ED) patterns indicative of two-dimensional crystalline self-assembly were obtained from samples, which were examined by cryo-electron microscopy, of monolayers of water-insoluble amphiphiles on vitrified aqueous substrates. The apparent hexagonal symmetry of an ED pattern from a $C_{16}H_{33}OH$ monolayer was interpreted in terms of multiple twinning. Monolayers of the $C_{31}H_{63}OH$ and cadmium salt of $C_{19}H_{39}CO_2H$ that were studied by dark-field techniques displayed faceted two-dimensional crystallites with a maximal size of 1 to 2 micrometers. Epitaxial nucleation of hexagonal ice by the $C_{31}H_{63}OH$ monolayer has also been demonstrated by ED.

Interfacial self-assembly of molecules into ordered two-dimensional (2D) aggregates is important to many fields (*1–3*), including crystal nucleation, the formation of mono- and multilayers, and molecular electronics. A method for the direct demonstration of such microscopic properties of amphiphilic monolayers in situ is grazing incidence x-ray diffraction (GIXD) by synchrotron radiation (*4*). This method has revealed that water-insoluble amphiphilic monolayers in the uncompressed, relaxed state are highly crystalline. This finding contrasts with the generally accepted view that monolayers need to be well compressed to exhibit 2D crystallinity. The GIXD method has allowed measurement of the structure and the growth and dissolution properties of self-aggregated monolayers as a function of parameters such as molecular length, temperature, solvent, and additives (*3*). Surface x-ray techniques do not yield direct images of the 2D crystal domains. Such domain morphologies have been examined by epifluorescence and Brewster angle microscopy. However, these methods are applicable only to domains larger than 1 μm in diameter and have not unambiguously revealed self-assembled monolayers on solutions displaying faceted 2D crystals (*5*). Atomic force microscopy has shown that domain structures in Langmuir monolayers of stearic acid, $C_{18}H_{39}CO_2H$, transferred from water onto polyethyleneimine-covered mica have fairly well faceted grains as small as 2 to 3 μm (*6*). Transmission electron microscopy (TEM) studies of mono- and multilayers of amphiphilic molecules that had been transferred (in a partially compressed state) from a water surface onto a solid support did not reveal submicrometer features in the domains (*7*).

The self-aggregating ability of amphiphilic monolayers on water suggests that one could fast-freeze the water subphase

---

J. Majewski, L. Margulis, D. Jacquemain, F. Leveiller, M. Lahav, L. Leiserowitz, Department of Materials and Interfaces, The Weizmann Institute of Science, 76100 Rehovot, Israel.
C. Böhm, Institut für Physikalische Chemie, Johannes Gutenberg Universität, D-6500 Mainz, Germany.
T. Arad, Department of Structural Biology, The Weizmann Institute of Science, 76100 Rehovot, Israel.
Y. Talmon, Department of Chemical Engineering, Technion–Israel Institute of Technology, Haifa 32000, Israel.

*To whom correspondence should be addressed.

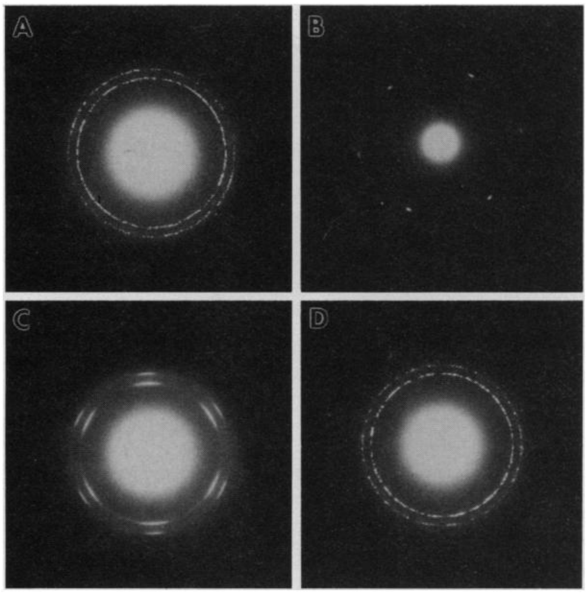

Fig. 1. Electron diffraction patterns, obtained from an area 3 µm in diameter, of four different monolayers on vitreous ice at −175°C. (**A**) A powder pattern from the monolayer of the carboxylic acid $C_{29}H_{59}CO_2H$. (**B**) Pattern from a single crystallite of the cadmium salt of the carboxylic acid $C_{19}H_{39}CO_2H$. (**C**) A diffraction pattern from the monolayer of the alcohol $C_{16}H_{33}OH$, which has been attributed to twinning. (**D**) A powder pattern from the monolayer of the alcohol $C_{31}H_{63}OH$. Halos of diffuse scattering from vitreous ice, corresponding to *d* spacings of 3.7 and 2.1 Å, were visible in the original negatives but too weak to be evident on the prints shown here.

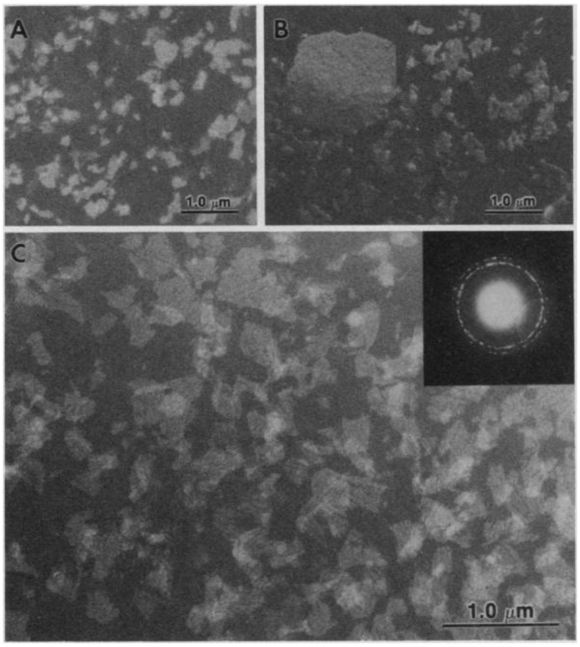

Fig. 2. Dark-field images of domains of monolayers at −175°C. (**A** and **B**) Different regions of the cadmium salt $C_{19}H_{39}CO_2H$ of the monolayer on vitreous ice. The relatively large domain of ~2 µm in (B) exhibits well-developed facets. (**C**) Domains of $C_{31}H_{63}OH$. Insert shows the position and size of the objective aperture used for dark-field imaging. There is some tendency for sixfold symmetry of the inner diffraction ring.

into vitreous ice and maintain the integrity of the relaxed monolayer. This procedure would allow measurement, almost in situ, by TEM. Many questions could then be addressed, such as whether 2D crystallites are faceted, how the domain structure depends on the growth history of the crystallite, and whether one may observe by lattice imaging the positions of heavy counterions bound to the monolayer. Langmuir monolayers have been used to induce the nucleation of three-dimensional (3D) crystals at the monolayer-solution interface by a structural complementarity (*1*). Therefore, it may be possible to obtain a combined electron diffraction (ED) pattern of the monolayer and underlying 3D crystal.

The fast cooling of aqueous solution substrates into vitreous ice (*8, 9*) has not been applied to the study of amphiphilic monolayers. We applied this method to a series of monolayers of fatty acids, fatty acid salts, and alcohols (*10*). These monolayers have already been shown by GIXD measurements as highly crystalline in the relaxed state (*2, 3*).

The ED pattern of $C_{29}H_{59}CO_2H$ shows three rings (Fig. 1A), which indicates that the monolayer crystallites are randomly arranged in a "powder" form. The *d* spacings corresponding to the three rings are 4.1, 3.7, and 2.5 Å, respectively (*11*). On the assumption that these three spacings correspond to the respective {1,1}, {0,2}, and {2,0} reflections, we deduced a rectangular unit cell of dimensions a = 5.0 Å and b =7.4 Å, giving an area per molecule ($ab/2$) of 18.5 Å^2. The $\{h,k\}$ assignment is consistent with the distribution of diffraction spots in Fig. 1A. The innermost ring displays far more spots than its outer neighbor, in accordance with a 2:1 multiplicity of the {1,1} and {0,2} reflections. Moreover, GIXD measurements from a monolayer of the same acid on water yielded a diffraction pattern that, when indexed as above, gave a structure at near atomic resolution (*12*). Finally, the derived cell dimensions indicate the presence of the herringbone motif found in 2D crystal structures of long hydrocarbon amphiphilic chains (*2*). The two molecular chains in such a unit cell are related by glide symmetry and are oriented so that the angle between their planes is ≈90°. This configuration results in a herringbone chain arrangement, generally specified as the orthogonal O⊥ motif (*13*).

A monolayer of the fatty acid $C_{19}H_{39}CO_2H$ was deposited on a 10^{-3} M aqueous solution of $CdCl_2$, in which the pH was adjusted to a value of 8.85 by the addition of NH_3. In the ED pattern from a single crystallite (Fig. 1B), the diffraction spots can be indexed as {1,1}, {0,2}, and {2,0} with *d* spacings of 4.0, 3.6, and 2.4 Å, respectively, defining a rectangular unit cell with dimensions (*14*) of a = 4.9 Å and b = 7.2 Å and an area per molecule of 17.6 Å^2. This low value for the area indicates that at −175°C the molecules are vertically aligned on the vitreous ice. A dark-field image of such a monolayer over the vitreous ice shows domains from 0.3 to 2 µm in size (Fig. 2, A and B). The largest domain appears to be well-faceted, but an assignment of all its facet angles in terms of the cell dimensions is ambiguous.

The monolayer of $C_{16}H_{33}OH$ on vitreous ice shows a highly symmetric hexagonal ED pattern (Fig. 1C) of six doublets. The *d* spacings of the inner and outer reflections of 4.1 and 3.6 Å may be indexed as {1,1} and {0,2}, respectively, to yield the rectangular unit cell of dimensions a = 5.0 Å and b = 7.2 Å. The GIXD data over pure water at 5°C yielded only the {1,1} reflection. The {0,2} reflection was too weak to be observed because of a low coherence length in that direction (*15*). The sixfold rotation symmetry of the ED pattern may be accounted for by the assumption that the crystallites twin about the {1,3} and {1,−3} planes (Fig. 3). This hypothesis is substantiated by the longer arcs of the {1,1} reflections compared to those of the {0,2} reflections, because the {1,3} diffraction vectors do not perfectly bisect the angle between the {1,1} and {0,2} diffraction vectors. We propose that the monolayer material deposited at room temperature exhibited threefold or sixfold symmetry in a partially ordered state. Cooling to 5°C produced

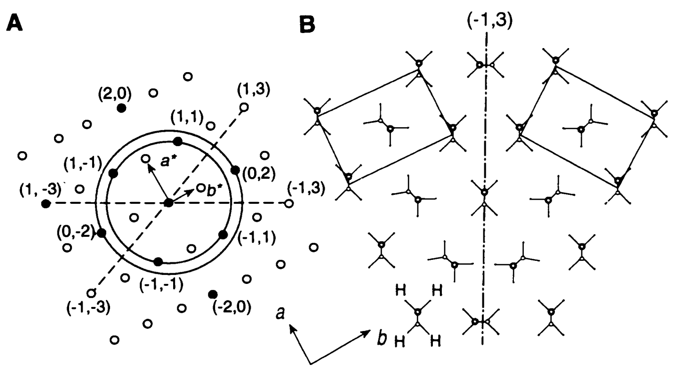

Fig. 3. (**A**) Reciprocal lattice of a single (untwinned) 2D crystal of $C_{16}H_{33}OH$ showing the observed (filled circles) and unobserved (empty circles) reflections. (**B**) A schematic view of a twinned packing arrangement of $C_{16}H_{33}OH$ about the {−1, 3} plane, yielding two segments. One way to rationalize the {−1,3} twinning plane is to note that the direction of strong interchain contacts, along the ***a-b*** axis, is almost maintained across the twinning plane. The $C_{16}H_{33}OH$ molecules are assumed to be vertically aligned, in keeping with the low area per molecule of 18.0 Å^2. The molecules are packed in plane symmetry group *p*1*g*1, where *p* represents a primitive unit cell and *g* represents a glide plane perpendicular to the *a* axis. The proposed structure of $C_{16}H_{33}OH$ is based on the fact that the alcohol chains $C_nH_{2n+1}OH$ (*n* = 16 to 31) pack in the orthogonal O⊥ motif on water at ~5°C, according to GIXD measurements.

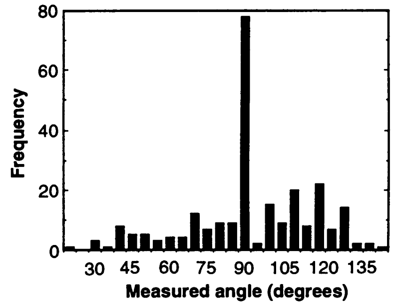

Fig. 4. Histogram of angles between well-defined facets of domains in the $C_{31}H_{63}OH$ monolayer. These values were taken from several dark-field micrographs, one of which is shown in Fig. 2C.

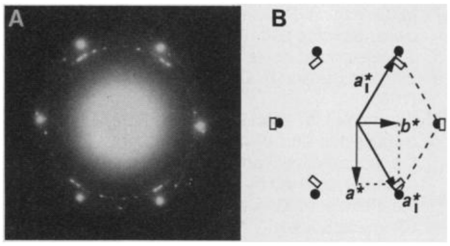

Fig. 5. (**A**) Electron diffraction pattern from an essentially single crystallite of the $C_{31}H_{63}OH$ monolayer on a single crystal of hexagonal ice showing their epitaxial relation: the six {1,0,0} diffraction vectors of hexagonal ice match well the four {1,1} and the two {0,2} vectors of the monolayer in both direction and magnitude. (**B**) The schematic relation between the reciprocal lattices of ice (filled circles) and of the monolayer (empty rectangles). Shown are ***a****, ***b****, and ***a****$_I$*, the base vectors of the reciprocal nets of the monolayer and hexagonal ice, respectively.

twinned crystallites of rectangular symmetry, in which the twinned sectors are related to each other by the threefold or sixfold point symmetry of the original crystallite. This result is in accord with Curie's principle that a physical event cannot have a symmetry lower than that of the event that caused it (*16*).

The typical ED pattern of monolayers of $C_{31}H_{63}OH$ on vitrified ice is shown in Fig. 1D. The rings may be indexed {1,1}, {0,2}, and {2,0} with respective *d* spacings of 4.2, 3.7, and 2.5 Å, yielding a rectangular unit cell with dimensions of *a* = 5.05 Å and *b* = 7.4 Å and an area per molecule of 18.7 Å^2. The diffraction rings indicate that the crystallites are randomly oriented azimuthally. The intensity distribution in the inner ring shows some tendency for sixfold symmetry (insert, Fig. 2C), indicative of partial twinning about the {1,3} directions. The dark-field image in Fig. 2C clearly shows crystallites of monolayer material in the size range between 0.5 to 1.0 μm. Many of these crystallites display polygonal morphology with well-defined facets. A histogram of the angles between facets with a common point (Fig. 4) shows an angular distribution that may be correlated with the angles between the planes of low-order {*h*,*k*} indices such as {1,0}, {0,1}, {1,1}, and {1,3}. The most prevalent angles are in the range of 90° ± 5°. This value may be attributed to the 90° angle between the {0,1} and {1,0} planes as well as the 92° angle between the {1,1} and {−1,2} planes. The relatively high proportion of angles in the region between 100° and 120° may arise from facets with indices of {1,1} and {1,−1} as well as {1,1} and {−1,3}.

The crystallites exhibit distinct striations (Fig. 2C), and the distances between neighboring striations vary from 0.1 to 0.3 μm. The possible directions of such striations may be deduced from the angle between the striation lines and the crystal facets. We have observed in several domains two specific configurations. In the first, the striations run parallel to an edge and the other facet is perpendicular to that edge. The second case involves two perpendicular edges, the striation making in most cases an angle of 35° to 40° with one of the edges. If the striation directions are the same in both cases, the only possibility for a striation direction is the {1,1} plane because the angle between the {1,1} and the {−1,2} planes is ≃90° and the angle between the {1,1} and {0,1} planes is ≃35°. These striations may have been introduced by the quenching of the monolayer solution. Because of the proposed commensurate character of the monolayer and hexagonal ice, the long-chain alcohols [$C_nH_{2n+1}OH$ (n > 23)] have been used to induce nucleation of the latter (*15*, *17*). According to GIXD measurements (*18*), $C_{31}H_{63}OH$ was found to maintain its 2D crystalline structure after nucleating hexagonal ice at the monolayer-water interface. To induce formation of hexagonal ice crystals under the monolayer, we cooled the water subphase slowly to the freezing point. An ED pattern shows the oriented superpositon of the {1,0,0} reflections of ice and the {1,1} and {0,2} reflections of the monolayer (Fig. 5).

The experimental results indicate that the structural and morphological properties of water-insoluble amphiphilic monolayers may be successfully studied on vitreous ice by TEM. Other possible applications include the study of 2D crystalline structures of proteins bound to amphiphilic monolayers (*19*) under almost in situ conditions. The evidence for the formation of ordered clusters of water-soluble amphiphiles at the solution interface is indirect (*1*, *2*). The ED technique may define the extent of lateral order in such systems. Finally, the observation of epitaxial growth of hexagonal ice by the alcohol monolayer suggests that other monolayer-matched systems may be examined in the same way.

REFERENCES AND NOTES

1. I. Weissbuch, L. Addadi, L. Leiserowitz, M. Lahav, *J. Am. Chem. Soc.* **110**, 561 (1988); E. M. Landau *et al.*, *Pure Appl. Chem.* **61**, 673 (1989); E. M. Landau, M. Levanon, L. Leiserowitz, M. Lahav, J. Sagiv, *Nature* **318**, 353 (1985).
2. D. Jacquemain *et al.*, *J. Am. Chem. Soc.* **113**, 7684 (1991); F. Leveiller *et al.*, *Science* **252**, 1532 (1991).
3. D. Jacquemain *et al.*, *Angew. Chem. Int. Ed. Engl.* **31**, 130 (1992).
4. J. Als-Nielsen and K. Kjaer, "Phase Transitions in Soft Condensed Matter," *Proceedings of the NATO Advanced Study Institute, Phase Transitions in Soft Condensed Matter*, T. Riste and D. Sherrington, Eds. (Plenum, New York, 1989), pp. 113–120.
5. A. Dietrich, H. Möhwald, W. Rellig, and G. Brezesinski [*Langmuir* **7**, 539 (1991)] observed by epifluorescence faceted domains as large as 30 μm of a compressed monolayer of a triple-chain lecithin. B. Berge, L. Fauchen, K. Schwab, and A. Libchaber [*Nature* **350**, 322 (1991)] observed domains of sodium dodecyl sulfate with facets as large as 50 μm on the water surface with concentrations, by weight, far below the critical micelle concentration, and so presumably of 2D crystals.
6. L. F. Chi, M. Anders, H. Fuchs, R. R. Johnston, H. Ringsdorf, *Science* **259**, 213 (1993).
7. M. Lösche *et al.*, *Thin Solid Films* **117**, 269 (1984);

A. Fischer and E. Sackman, *Nature* **313**, 299 (1985); A. Fischer, M. Lösche, H. Möhwald, E. Sackmann, *J. Phys. Lett.* **45**, L-785 (1984); A. Fischer and E. Sackmann, *J. Phys.* **45**, 517 (1984).

8. J. Dubochet, J. Lepault, R. Freeman, J. A. Berriman, J.-C. Homo, *J. Microsc.* **128**, 219 (1982); J. Lepault, F. P. Booy, J. Dubochet, *ibid.* **129**, 89 (1983); M. Adrian, J. Dubochet, J. Lepault, A. W. McDowall, *Nature* **308**, 32 (1984); J. Dubochet *et al.*, *Rev. Biophys.* **21**, 129 (1988).
9. J. L. Burns, Y. Cohen, Y. Talmon, *J. Phys. Chem.* **94**, 5308 (1990); A. Walter, P. K. Vinson, A. Kaplun, Y. Talmon, *Biophys. J.* **60**, 1315 (1991); R. G. Laughlin, R. L. Munyon, J. L. Burns, Y. Talmon, *J. Phys. Chem.* **96**, 474 (1992); N. Kamenka, M. Chorro, Y. Talmon, R. Zana, *Colloids Surf.* **67**, 213 (1992); R. Zana and Y. Talmon, *Nature* **362**, 228 (1993).
10. Collodion-carbon–coated grids of 400 mesh, prepared according to a conventional technique [W. Baumeister and M. Hahn, in *Principles and Techniques of Electron Microscopy*, M. Hayat, Ed. (Van Nostrand Reinhold, New York, 1978), pp. 21–33 and 37–46], were placed on a stainless steel mesh in a specially prepared Teflon trough under the water subphase. Monolayers were spread (~70% available surface) on the surface of an aqueous solution at 20°C. The subphase was then cooled to 5°C, a temperature at which GIXD studies have shown the uncompressed monolayers to be highly crystalline. The water subphase was slowly drained with a motor-driven syringe, and the grids with the deposited monolayers were transferred to the plunging device [J. R. Bellare, H. T. Davis, I. F. Scriven, Y. Talmon, *J. Electron Microsc. Tech.* **10**, 87 (1988)]. Excess water on the underside of the grid was blotted with filter paper, and the grids were rapidly plunged into liquid ethane cooled by liquid nitrogen to its freezing point. Such fast cooling has been found to vitrify the aqueous subphase, that is, to inhibit ice crystallization. The specimens were loaded into a Gatan 626 cold stage and examined in a Philips CM12 transmission electron microscope operated at 100 kV. The grids were maintained at -175°C throughout their examination, and dark-field technique was applied to obtain images of individual domains. To minimize radiation damage, low-dose precautions were used. However, even under low-dose conditions the specimens remained intact for 10 s or less.
11. Observed reflections from hexagonal ice, albeit rare, were used to calibrate the camera length and so permit the *d* spacings to be determined with sufficient accuracy.
12. F. Leveiller, D. Jacquemain, L. Leiserowitz, K. Kjaer, J. Als-Nielsen, *J. Phys. Chem.* **96**, 10380 (1992).
13. D. M. Small, in *Handbook of Lipid Research* (Plenum, New York, 1986), vol. 4, chaps. 2, 4, 5, and 8.
14. The maximum error in the determination of the unit cell dimensions is ~5%.
15. R. Popovitz-Biro *et al.*, unpublished data.
16. P. Curie, *J. Phys.* **3**, 393 (1894).
17. M. Gavish, R. Popovitz-Biro, M. Lahav, L. Leiserowitz, *Science* **250**, 973 (1990).
18. J. Majewski *et al.*, unpublished data.
19. E. E. Uzgiris and R. D. Kornberg, *Nature* **301**, 125 (1983).

20. We thank I. Weissbuch and R. Popovitz-Biro for discussions and J. Als-Nielsen and K. Kjaer for the cooperative venture into the GIXD experiments. Supported by the Minerva Foundation and the Petroleum Research Fund of the American Chemical Society.

16 March 1993; accepted 23 June 1993

Early and Late Alkali Igneous Pulses and a High-^{3}He Plume Origin for the Deccan Flood Basalts

Asish R. Basu, Paul R. Renne, Deb K. DasGupta,
Friedrich Teichmann, Robert J. Poreda

Several alkalic igneous complexes of nephelinite-carbonatite affinities occur in extensional zones around a region of high heat flow and positive gravity anomaly within the continental flood basalt (CFB) province of Deccan, India. Biotites from two of the complexes yield ^{40}Ar/^{39}Ar dates of 68.53 ± 0.16 and 68.57 ± 0.08 million years. Biotite from a third complex, which intrudes the flood basalts, yields an ^{40}Ar/^{39}Ar date of 64.96 ± 0.11 million years. The complexes thus represent early and late magmatism with respect to the main pulse of CFB volcanism 65 million years ago. Rocks from the older complexes show a ^{3}He/^{4}He ratio of 14.0 times the air ratio, an initial ^{87}Sr/^{86}Sr ratio of 0.70483, and other geochemical characteristics similar to ocean island basalts; the later alkalic pulse shows isotopic evidence of crustal contamination. The data document 3.5 million years of incubation of a primitive, high-^{3}He mantle plume before the rapid eruption of the Deccan CFB.

A common model for the origin of CFB provinces is that they are generated by mantle plumes (*1*). In this model, partial melting initiated by the arrival of the hot plume thins and conductively heats the lithosphere. Further rise of the plume through the lithosphere causes rapid eruption of the CFB (*2, 3*). The distinct geochemical and isotopic signatures of the CFB (*4*) support such a plume origin, although others have suggested (*5*) an upper mantle or lithospheric source for CFB. In this report, we provide age and geochemical evidence from three of the alkalic igneous complexes of the Deccan trap CFB of peninsular India that document the chemical evolution of this rising plume through the continental lithosphere over a 3.5-million-year time interval.

The western Indian crustal plate can be divided into a number of segments separated by fracture zones radiating from the Cambay basin (Fig. 1), an area of high heat flow associated with well-defined positive gravity anomalies (*6, 7*). A number of alkali-carbonatite bodies associated with the Deccan tholeiites crop out along the Narmada Valley, a rift extending eastward from the Cambay basin (Fig. 1), and along another prominent fault zone parallel to the western coast of India, extending through the Cambay basin possibly as much as 600 km to the north (*8*). This fault zone also contains alkalic rocks of the Bombay area (*9*). The Girnar (*10*) and the Phenai Mata (*11*) alkali complexes, all volcanic plugs, follow essentially an east-west trend (Fig. 1). A connection between the Maldive ridge, an oceanic north-south lineament off the west coast, and the Deccan Traps in the mainland is indicated by seismic refraction profiles of the western Indian Ocean (*12*). The Sarnu-Dandali and Mundwara alkalic complexes (Fig. 1) are situated approximately at the northward extension of the Maldive ridge through the West Coast fault, Panvel Flexure, and the Cambay Graben. Drilling in the gravity high near Kadi in the Cambay basin has recovered nepheline syenite at the base of the Tertiary sediments (*13*). The alkali rocks of Sarnu and Mundwara (*14*) and Kadi may be aligned along a zone extending to the southern end of the Cambay basin; the alkalic plugs and flows of central Kutch (Fig. 1) may also belong to a zone connecting this basin. These correlations indicate that the Deccan province extends beyond the present-day boundaries of the traps (Fig. 1), particularly to the north.

The Mundwara magmatic complex (Fig. 1) occurs as ring-shaped and plug-like intrusions within the Erinpura granite of Proterozoic age in Rajasthan (24°50′N, 72°33′E). Two units of the complex, Toa and Mer, show arcuate, ring-shaped hills (2 to 3 km in diameter), whereas the third, Musala, is a single conical hill about 1 km in diameter (*15, 16*). Ultramafic and mafic rocks are dominant in the Toa complex; the Mer intrusion is composed mostly of alkaline mafic rocks. Mafic rocks also dominate the Musala plug, but some felsic rocks, such as foid syenites and foid monzosyenites, are also present. All three intrusions have chilled margins and contain many dikes of diabase, basalts, microsyenites, phonolites, and lamprophyres. In addition, carbonatite dikes intrude rocks outside the Mer ring. The distribution of alkaline mafic rocks and syenites in association with more mafic and ultramafic differentiates, such as picrites and pyroxenites, implies that all these rock

A. R. Basu, F. Teichmann, R. J. Poreda, Department of Geological Sciences, University of Rochester, Rochester, NY 14627.

P. R. Renne, Institute of Human Origins, Geochronology Center, Berkeley, CA 94709.

D. K. DasGupta, Department of Geology, Presidency College, Calcutta, India 700073.